

A high-resolution, spatially explicit estimate of fossil-fuel CO₂ emissions from the Tokyo Metropolis, Japan

Richao Cong (✉ richao.cong@nies.go.jp)

National Institute for Environmental Studies <https://orcid.org/0000-0002-6315-6147>

Makoto Saito

National Institute for Environmental Studies

Tetsuo Fukui

Institute of Behavioral Sciences

Ryuichi Hirata

National Institute for Environmental Studies

Akihiko Ito

National Institute for Environmental Studies

Methodology

Keywords: Carbon dioxide, CO₂ emission inventory, Fossil fuel, GIS, High-resolution map, Tokyo emissions

Posted Date: June 4th, 2020

DOI: <https://doi.org/10.21203/rs.3.rs-17565/v2>

License:  This work is licensed under a Creative Commons Attribution 4.0 International License.

[Read Full License](#)

1 **A high-resolution, spatially explicit estimate of fossil-fuel CO₂**
2 **emissions from the Tokyo Metropolis, Japan**

3 Richao Cong^{1,2*}, Makoto Saito^{1*}, Tetsuo Fukui³, Ryuichi Hirata¹ and Akihiko Ito¹

4 ¹ Center for Global Environmental Research, National Institute for Environmental Studies,
5 Tsukuba, Japan

6 ² Fukushima Branch, National Institute for Environmental Studies, Tamura District, Japan

7 ³ Institute of Behavioral Sciences, Tokyo, Japan

8 **Correspondence:*

9 richao.cong@nies.go.jp; saito.makoto@nies.go.jp

10 **Abstract**

11 **Background:** The quantification of urban greenhouse gas (GHG) emissions is an important
12 task in combating climate change. Emission inventories that include spatially explicit
13 emission estimates facilitate the accurate tracking of emission changes, identification of
14 emission sources, and formulation of policies for climate-change mitigation. Many currently
15 available gridded emission estimates are based on the disaggregation of country- or state-
16 wide emission estimates, which may be useful in describing city-wide emissions but are of
17 limited value in tracking changes at subnational levels. Urban GHG emissions should
18 therefore be quantified with a true bottom-up approach.

19 **Results:** Multi-resolution, spatially explicit estimates of fossil-fuel carbon dioxide (FFCO₂)
20 emissions from the Tokyo Metropolis, Japan, were derived. Spatially explicit emission data
21 were collected for point (e.g., power plants and waste incinerators), line (mostly traffic), and
22 area (e.g., residential and commercial areas) sources. Emissions were mapped on the basis of
23 emission rates calculated for source locations. Activity, emissions, and spatial data were
24 integrated, and the results were visualized using a geographic information system approach.

25 **Conclusions:** The annual total FFCO₂ emissions from the Tokyo Metropolis in 2014 were
26 44,855 Gg CO₂, with the road-transportation sector (16,323 Gg CO₂) accounting for 36.4% of
27 the total. Spatial emission patterns were verified via a comparison with the East Asian Air
28 Pollutant Emission Grid Database for Japan (EAGrid-Japan), which demonstrated the
29 applicability of this methodology to other prefectures and therefore the entire country.

30

31 **Keywords:** Carbon dioxide, CO₂ emission inventory, Fossil fuel, GIS, High-resolution map,
32 Tokyo emissions

33 **Background**

34 Fossil-fuel combustion is a major contributor to increasing atmospheric carbon dioxide (CO₂)
35 concentrations [1], with cities worldwide being responsible for more than 70% of the global
36 total fossil-fuel CO₂ emissions (FFCO₂) [2]. As large sources of FFCO₂, cities have great
37 potential for emission mitigation [3]. In response to the need for local climate action, many
38 global cities have participated in climate action groups, such as the C40 Cities Climate
39 Leadership Group [4] and the Global Covenant of Mayors for Climate & Energy [5], and
40 started compiling emission inventories (EIs). The EIs are often compiled following the
41 Global Protocol for Community-Scale Greenhouse Gas Emission Inventories (GPC) [6].
42 The Paris Agreement of the United Nations Framework Convention on Climate Change
43 (UNFCCC) recognizes the importance of climate-change mitigation at subnational levels [7].
44 However, subnational emission estimates (e.g., state, province, city (UN-Habitat [2]), and
45 private sector) are beyond the scope of the current Intergovernmental Panel on Climate
46 Change (IPCC) guidelines. The inventory framework implemented under the Kyoto Protocol
47 focuses on national compliance with global emission-reduction targets [8], rather than
48 monitoring emission changes at subnational levels.

49 Subnational emission estimates can be obtained from spatially explicit emission data. Gurney
50 et al. [9] loosely categorized emission modeling approaches as ‘downscaled’ or

51 ‘mechanistic’. In general, emission estimates using mechanistic approaches are more suitable
52 for tracking emission changes in local areas. For example, emissions in the National
53 geoinformation technologies, temporospatial approaches, and the Protocol for Reducing
54 GHG Emission Uncertainties (GESAPU) are calculated at the locations of sources (e.g.,
55 points, lines, and areas), taking into account the emission processes [10]. Thus, GESAPU
56 estimates can be used to keep track of local emission changes over the domain of a single
57 country. In the US, Gurney et al. have developed city-scale emission data for several cities,
58 including Indianapolis [11], Los Angeles [12], Salt Lake City [13], and Baltimore [14] under
59 the Hestia Project. In Japan, Mori [15] developed a multi-resolution fossil-fuel CO₂ emission
60 model for Osaka.

61 This paper presents the first spatially explicit FFCO₂ emission data for the Tokyo Metropolis
62 (population 13.6 M in 2016; area 2,189 km²) for the year 2014. We distinguish our work
63 from the East Asian Air Pollutant Emission Grid Database for Japan (EAGrid-Japan) by the
64 use of a multi-resolution approach and updated information. We describe varieties of
65 statistical and geospatial data used in estimating and mapping emissions, and compare our
66 emission estimates with existing estimates at aggregated city and grid cell levels. We also
67 discuss current limitations and future improvements.

68

69 **Methods**

70 **Emission definition and modeling framework**

71 The focus here is on quantifying FFCO₂ emissions from the Tokyo Metropolis using the
72 modeling framework described in Fig. 1. Following previous studies [10, 11, 15], a multi-
73 resolution emission modeling approach was employed, where CO₂ emissions (‘emissions’
74 hereinafter) were calculated on an individual source basis in a bottom-up manner, rather than
75 using aggregated emission-sector levels. Emissions were spatially allocated using verified
76 geographic latitude and longitude coordinates (mainly for point sources) and spatial
77 geolocation data (for line and area sources), with examples of point-source locations and
78 geospatial data shown in Fig. 2.

79 The total emissions for the year 2014 were calculated using the best available locally
80 collected data following the 2006 IPCC guidelines [16]. Emission sources therefore included
81 electricity generation (IPCC code 1A1ai), civil aviation (1A3a), waterborne navigation
82 (1A3d), waste incineration (4C1), road transportation (1A3bi, 1A3bii, and 1A3biii), industrial
83 and commercial sources (1A1aiii, 1A2, 1A4a, and 1A4ciii), residential sources (1A4b), and
84 agricultural machine use (1A4cii). These emissions were calculated using the Tier 3 approach
85 [16]. The emission-sector definitions, spatial information and data, activity data, and
86 emission factors are summarized in Table 1.

87

88 **Point-source emissions**

89 Point-source emissions include those from electricity generation, civil aviation, waterborne
90 navigation, and waste incineration (Table 1). For electricity generation, only fossil-fueled
91 power plants in Tokyo ($n = 19$) were considered (see Additional File 1; Table S1 for details).
92 The 2014 total emissions from all power plants were calculated by formula:

$$93 \quad E_{eg} = 24 \cdot \sum_{i=1}^n \sum_{j=1}^{12} C_i \cdot D_j \cdot R_{g,j} \cdot EF_{g,j}, \quad (1)$$

94 where E_{eg} represents the total annual emissions from electricity generation (Gg CO₂); the
 95 coefficient 24 indicates the number of hours per day; C_i is the electricity generation capacity
 96 (kW) of power plant i in Tokyo with one type of generator (steam, gas cogeneration, or
 97 internal combustion); D_j is the number of days in month j ; $R_{g,j}$ is the mean operating ratio of
 98 fossil-fueled power plants with generator type g in month j for 2014; and $EF_{g,j}$ is the
 99 emission factor for fossil-fueled electricity generation by generator type g in month j (Gg
 100 CO₂ kWh⁻¹). The C_i values were obtained from the Electrical Japan Database (data were
 101 collected in April 2017) [17] and operator companies [18–20]. The $R_{g,j}$ values are reported
 102 by power plant operators and published by the government of Japan each year [21]. The
 103 emission factors of power plants in 2014 ($EF_{g,j}$) were derived from electricity generation
 104 amounts by power plants, the monthly fuel consumption (e.g., coal, crude oil, heavy oil, light
 105 oil, liquefied natural gas, liquefied petroleum gas, and other gas) [22], and official guidelines
 106 for GHG emissions counting [23]. Where there was a lack of individual data for a plant, R_j
 107 and EF_j values for plants with the same type of generator were used. The stack centroid was
 108 used as the representative emission location for multiple smoke stacks in a single power plant
 109 facility. An example of point-source emissions in SG Ward (see Table S2) is shown in Fig.
 110 2A.

111 Civil aviation emissions included those from passenger and cargo aircraft during landing and
 112 take-off (LTO) at an international airport, four helipads, and six domestic airports (Table S1).
 113 The 2014 total emissions from LTO movements were calculated as follows:

$$114 \quad E_{ca} = 2 \cdot \sum_{i=1}^n \sum_a F_{a,i} \cdot N_a \cdot EC_e \cdot EF_f, \quad (2)$$

115 where E_{ca} represents the total annual emissions from civil aviation (Gg CO₂); $F_{a,i}$ is the total
 116 number of arrivals for type a aircraft with one type of engine at airport i in 2014 (the
 117 coefficient 2 indicates landings = departures in LTO cycles); N_a is the number of engines on
 118 type a aircraft; EC_e is the jet fuel (‘energy’) consumption per engine during an LTO cycle by
 119 engine type e (Gg per engine per LTO); and EF_f is the emission factor of jet fuel (3.154 Gg
 120 CO₂ Gg⁻¹) [23]. The $F_{a,i}$ and N_a values were summarized from 2014 flight records [24–32]
 121 and websites [33]. The monthly proportion of aircraft types at Haneda airport was used as the
 122 annual proportion for 2014 due to the lack of annual flight timetables for each aircraft type.
 123 The monthly proportions of arrivals for each aircraft type were obtained from flight
 124 timetables for April 2017 [34, 35]. The EC_e values were extracted from the Aircraft Engine
 125 Emissions Databank of the International Civil Aviation Organization (ICAO) [36] and
 126 guidance on helicopter emissions [16, 37]. As aircraft are mobile sources, the calculated
 127 emissions were mapped using representative points on airport runways (diameter ~1 km) as
 128 point sources.

129 Emissions from the waterborne navigation sector included emissions from fuel consumed by
 130 vessels during round trips to ports in Tokyo ($n = 15$; Table S1). The 2014 total emissions
 131 from vessels were calculated as follows:

$$132 \quad E_{wn} = \sum_{i=1}^n \sum_{t,m} I_{t,m} \cdot R_{t,m} \cdot T_{t,m} \cdot N_{t,i} \cdot EF_t, \quad (3)$$

133 where E_{wn} represents the total annual emissions by vessels (Gg CO₂); $I_{t,m}$ is the emission
 134 intensity of fuels (tonne per vessel) for type t vessels (including merchant vessels, car ferries,
 135 evacuation vessels, fishing vessels, and other vessels) at mode m (travelling, mooring, cargo

136 loading, and unloading); $R_{t,m}$ is the load factor of type- t vessels in mode m ; $T_{t,m}$ is the fuel
 137 consumption time of type- t vessels in mode m (h); $N_{t,i}$ is the annual number of type- t vessels
 138 travelling to port i ; and EF_t is the emission factor (Gg CO₂ tonne⁻¹) for type- t vessels
 139 consuming heavy oil or light oil. The $I_{t,m}$, $R_{t,m}$, and $T_{t,m}$ values and the average travel speed
 140 for these vessels were obtained from technical reports [38, 39]. As shown by the parameters
 141 listed in Table S3, the mean travel distance was assumed to be 1 km in travelling mode to
 142 derive the travel time. The emissions from travelling mode were considered for fishing
 143 vessels but all mode were considered for the other types of vessels. The $N_{t,i}$ values were
 144 obtained from statistical data on vessels in ports [40, 41]. The EF_t data were extracted from
 145 the official guideline [23]. As waterborne vessels are mobile sources, representative points on
 146 port buildings were used as their point-source locations.

147 Emissions from incineration plants do not contribute to FFCO₂ emissions. However, this
 148 study included their emissions because the emission intensity is significant. Emissions from
 149 incineration plants for municipal solid waste (MSW, $n = 46$) and industrial waste ($n = 15$)
 150 (Table S1) included those from the combustion of wastes containing carbon (e.g., papers,
 151 plastics, textiles, rubbers, and oil) and the combustion agent (CA, “city gas” comprising
 152 liquid petroleum gas and natural gas). Emissions from MSW waste combustion were
 153 calculated as follows:

$$154 \quad E_{mww} = \sum_{i=1}^n (\sum_c T_i \cdot R_{c,i} \cdot FC \cdot EF_c + T_i \cdot CR \cdot EF), \quad (4)$$

155 where E_{mww} represents the 2014 total emissions from MSW incineration (Gg CO₂); T_i is the
 156 total amount of combustible content in waste (tonne) incinerated annually at plant i ; $R_{c,i}$ is
 157 the proportion of type- c content of waste (i.e., waste paper, plastic, rubber, and textiles in
 158 MSW) at plant i ; FC is the fossil carbon content in waste; EF_c is the emission factor for
 159 combustible content type c in waste (paper 1.69×10^{-5} ; plastic 2.55×10^{-3} ; textiles 2.29×10^{-3} ;
 160 rubber 1.72×10^{-3} Gg CO₂ tonne⁻¹) [23]; CR is the mean consumption of CA (1.29 m^3
 161 tonne⁻¹) [42]; and EF is the emission factor for CA (2.21×10^{-6} Gg CO₂ m⁻³) [23]. The T_i
 162 and $R_{c,i}$ values for all 46 MSW incineration plants in Tokyo were obtained from the
 163 investigation report on MSW for Tokyo, 2014 [43]. Here we assumed that paper and textiles
 164 in wastes were in equal amounts and the fossil carbon content (FC) of these wastes were
 165 50%. The CR values derived from available data for 19 MSW incineration plants in Tokyo
 166 [42] were used for all MSW incineration plants.

167 Emissions from industrial waste combustion were calculated as follows:

$$168 \quad E_{iww} = \sum_c T_c \cdot FC \cdot EF_c, \quad (5)$$

169 where E_{iww} represents the 2014 total emissions from industrial waste incineration (Gg CO₂);
 170 T_c is the total annual amount of combustible content in waste (tonnes) at all plants in Tokyo
 171 for type c (i.e., waste paper, plastic, textiles, and oil in industrial waste); and EF_c is the
 172 emission factor for fossil carbon in waste type c (oil 2.92×10^{-3} Gg CO₂ tonne⁻¹) [23]. T_c
 173 values were extracted from the investigation report on industrial waste incineration [44]. The
 174 FC value for industrial waste was assumed to be 1 with no CA used due to the high-purity
 175 carbon content. The emissions from 15 industrial-waste incineration plants were derived by
 176 allocating the E_{iww} with plant disposal capacities [45]. The central points of the chimneys at
 177 waste incineration plants were mapped as emission points.

178

179 **Line-source emissions**

180 Line-source emissions included those of the road-transport sector, based on traffic census
181 data compiled by the Ministry of Land, Infrastructure, Transport and Tourism for each
182 prefecture every five years, with the latest being in 2015 [46]. The census data include road
183 information (name, width, length, number of lanes, and classification for each road segment),
184 hourly and daily traffic volumes, and 12-h mean daytime vehicle speeds for small vehicles
185 (light passenger cars, regular passenger cars, light trucks, and small freight cars) and large
186 vehicles (bus, regular truck, and special-use vehicles). The road segment data indicate the
187 network links, as shown in the example of a digital road map (DRM; [47]) in Fig. 2B. The
188 census targets five road classifications: high-speed national highways, urban highways,
189 general national highways, major regional roads (prefectural roads and designated city roads),
190 and general regional roads. Emissions on minor roads that were not covered by the census
191 were not considered.

192 Road transportation emissions were calculated for single road segments ($n = 45,564$) as
193 follows:

194
$$E_{rt} = \sum_{i=1}^n \sum_v Q_{v,i} \cdot L_i \cdot EF_{v,s}, \quad (6)$$

195 where E_{rt} represents the 2014 total emissions from road transportation (Gg CO₂); $Q_{v,i}$ is the
196 annual traffic volume (derived from daily data) for type v vehicles at a vehicle speed (from 5
197 to 90 km/h) on road segment i ; L_i is the length of road segment i (km); $EF_{v,s}$ is the emission
198 factor for type- v vehicles by vehicle speed s (Gg CO₂ km⁻¹ per vehicle). The census
199 identification numbers for road segments were used with Google Maps software to select
200 point coordinates for each observed road segment, with the selected points being mapped to
201 identify the same roads on the DRM. The information from the traffic census, such as road
202 classification, daily traffic volume, and mean speed, were combined for the DRM road
203 segments. The average traffic conditions for each road classification in each municipality unit
204 [48] were substituted for the road segments not covered by the census. The L_i values were
205 calculated from the DRM using a geographic information system (GIS) tool. The $EF_{v,s}$ values
206 were obtained from Dohi et al. [49] (Table 2). Emissions were mapped on the center line of
207 each road segment.

208

209 **Area-source emissions**

210 Area-source emissions included those from the industrial, commercial, residential, and
211 agricultural sectors. The main source of industrial, commercial, and residential emissions is
212 fuel consumption in buildings, for which the Hestia project [14] estimated non-electrical
213 energy using the eQUEST simulation tool [50] by incorporating the building classification
214 and age, with the building emissions based on the building total floor areas (TFAs) [51].
215 Since spatial data (building polygons) are not available for buildings of all ages in Japan,
216 census data were used to allocate the emissions using building polygons (Fig. 2C) based on
217 the TFAs.

218 Emissions from the industrial and commercial sector included those from fossil-fuel
219 consumption by workers. Emissions from all areas in Tokyo, based on the economic census
220 ($n = 5,318$), were calculated as follows:

221
$$E_{ic} = \sum_{i=1}^n \sum_q W_{q,i} \cdot \frac{TE_q}{TW_q}, \quad (7)$$

222 where E_{ic} represents the 2014 total emissions from the industrial and commercial sector (Gg
 223 CO₂); $W_{q,i}$ is the number of workers for category q in census area i (Table 3); TE_q is the total
 224 annual emissions for category q (Gg CO₂); and TW_q is the total number of workers in category
 225 q . The $W_{q,i}$ values for all of the categories in census areas were obtained from the 2014
 226 economic census [52]. The census area comprised politically based blocks with an average area
 227 of around 0.5 km². The TW_q values were obtained from economic census data [52], and the
 228 TE_q values were extracted from the Tokyo energy-balance table [53]. The annual CO₂ emission
 229 factors by workers ($\frac{TE_q}{TW_q}$; Gg CO₂ per worker) were derived for each category (Table 3). The
 230 annual emissions from the fuels used in energy conversion (e.g., electricity generation and
 231 waste incineration) were not included in the energy-balance table [53] to avoid counting them
 232 twice. The total emissions for the industrial and commercial sector were allocated to every
 233 census area, similar to the approach used by Gately and Hutyra (2017) [54] with commercial
 234 emissions.

235 Total emissions were allocated to individual buildings in each census area, with all of the
 236 building polygons being associated to a given building use (industrial and commercial, or
 237 residential), using land-use maps covering four areas (23 wards in Tokyo, the Tama city area,
 238 Tama rural area, and island areas) at spatial resolutions of 3 × 3 m to 43 × 43 m [55]. The
 239 data on individual building polygons (e.g., site area (m²), height (m), number of floors, and
 240 floor area (m²)) were obtained as follows. Each building site area was estimated from the
 241 building polygon maps, and the building height was estimated from the difference in heights
 242 between a raster-type digital surface model (DSM) [56] and a vector-type digital-elevation
 243 model (DEM) [57]. DSM v. 1.1 was based on digital photos from the Advanced Land
 244 Observing Satellite, with an accuracy within 5 m [56]. A 30 × 30 m DSM dataset was used
 245 with a 5 × 5 m DEM dataset (updated in 2016) based on airborne laser observations (2015),
 246 with an elevation accuracy within 0.7 m (standard deviation) [57]. The number of floors was
 247 estimated by dividing the building height by the average ceiling height (2.9 m for residential
 248 buildings, and 3.5 m for industrial and commercial buildings). The TFAs were estimated by
 249 multiplying the site area by the number of floors. The emission factors of the buildings (Gg
 250 CO₂ m⁻²) in each census area were calculated by dividing the total emissions by the TFAs,
 251 aggregated over the census areas. Finally, the emissions from each industrial and commercial
 252 building were estimated by multiplying the emission factors by the TFAs of the individual
 253 buildings. Industrial and commercial emissions were mapped at the level of individual
 254 buildings.

255 Emissions from the residential sector were calculated for all of the population census areas in
 256 Tokyo ($n = 5,578$) by formula:

$$257 \quad E_{re} = \sum_{i=1}^n \sum_{f,h,b} A_{h,b,i} \cdot EF_{f,h,b}, \quad (8)$$

258 where E_{re} represents the 2014 total emissions from the residential sector (Gg CO₂); $A_{h,b,i}$ is
 259 the number of households with occupancy h (with four categories: 1, 2, 3, or ≥4 occupants) in
 260 type b buildings (collective or detached) in the census area i ; and $EF_{f,h,b}$ is the total annual
 261 emission intensity (Gg CO₂ yr⁻¹ per household) of fuel type f , in household with occupancy
 262 h , and for building type b . The $A_{h,b,i}$ values were obtained from the 2015 population census
 263 data [58], and the $EF_{f,h,b}$ were from an investigation report on energy consumption in

264 households as provided in Table 4 [59]. Finally, the total emissions from each census area
265 were allocated to each building in proportion to the TFAs and with consideration of whether
266 the buildings were collective or detached, and mapped at the level of individual buildings.
267 Agricultural emissions in this study are defined as emissions from fossil fuel use in
268 agricultural machinery. The emissions processes were considered as those arising during crop
269 planting, and those associated emissions were calculated for 62 municipalities in Tokyo as
270 follows:

$$E_{am} = \sum_{i=1}^n \sum_p A_{p,i} \cdot EF_p, \quad (9)$$

271
272 where E_{am} represents the 2014 total emissions from agricultural machinery use (Gg CO₂); $A_{p,i}$
273 is the area for crop type p cultivated in municipality i (ha); and EF_p is the annual emission
274 factor for farmland by crop type (Gg CO₂ ha⁻¹). The $A_{p,i}$ value for each Tokyo municipality
275 was obtained from the agricultural census [60] and an investigation report on agricultural
276 products in Tokyo [61], and the EF_p values were from a 2003 report [62] and an academic
277 paper [63] (Table 5). Farmland was divided into two categories, rice paddy fields and other
278 farmland, using a land-use map at a 10 × 10 m spatial resolution based on remote-sensing data
279 for the 2006–2011 period [64]. Finally, the agricultural emissions mapped in each municipality
280 [48] were sorted into a 10 × 10 m mesh for mapping based on the two types of farmland.

281

282 Data integration

283 Emission calculations and spatial emissions mapping/modeling were integrated using ArcGIS
284 v. 10.4. The world geodetic system (1984) was used for mapping all of the emission sources,
285 and a symbol tool was used here for visualizing the emissions on maps. A 3D map of the
286 emission sources in SG Ward is shown in Fig. 2D as an example, allowing visualization of
287 the emissions from local facilities, road segments, and buildings.

288 All of the data used, their versions or editions, and sources are summarized in Table S4. More
289 than two million building polygons were used to produce emission maps around 500 MB in
290 size. The emission maps were not gridded products since a multi-resolution approach was
291 adopted. The original maps were converted to a 1 km mesh size (Fig. 3) for convenience in
292 data handling.

293

294 Results and discussion

295 Total emissions from the Tokyo Metropolis

296 Tokyo is one of 47 prefectures in Japan and comprises 23 central city wards and multiple
297 cities, towns, and villages (Table S2). The three highest point-source gridded emissions in
298 2014 occurred in SG, OT, and MN Wards at 6,183, 1,814, and 253 Gg CO₂ km⁻²,
299 respectively (Fig. 3A), due to two large power plants and a major airport being located within
300 these areas. The highest line-source emissions occurred in KT, OT, and EG Wards at 155,
301 146, and 144 Gg CO₂ km⁻², respectively (Fig. 3B). The highest gridded emissions for area
302 sources (Fig. 3C) occurred in CD, CO, and SJ Wards at 173, 168, and 164 Gg CO₂ km⁻²,
303 respectively. These high emissions are primarily due to the high floor numbers and large
304 building areas for residential, industrial, and commercial use concentrated in these areas. A
305 total emissions map is given in Fig. 3D, with the three highest emissions being 6,210 in SG
306 Ward, 1,965 in OT Ward, and 295 Gg CO₂ km⁻² in MN Ward, respectively.

307 The estimated total 2014 FFCO₂ emissions from Tokyo were 44,855 Gg CO₂ (Table 6),
308 which comprised individual sector contributions of 16,323 from road transportation; 13,085
309 from the industrial and commercial sector; 6,478 from electricity generation; 5,302 from the
310 residential sector; 1,879 from civil aviation; 1,483 from waste incineration; 279 from
311 waterborne navigation; and 26 Gg CO₂ from the agricultural machine use sector. Total annual
312 emissions from the area, line, and point sources were 18,413, 16,323, and 10,119 Gg CO₂,
313 respectively.

314 The highest point-source emissions (Fig. 4) for 2014 were as follows. Power plants:
315 Shinagawa (3,219), Oi (2,965), and Roppongi energy service (140 Gg CO₂) plants; Civil
316 aviation: Haneda (1,814), Chofu (30), and Oshima (8 Gg CO₂) airports; Waterborne
317 navigation: Tokyo (253), Mikurajima (5), and Okada (4 Gg CO₂) ports; and waste
318 incineration plants: Tokyo Waterfront Recycle Power (188), Koto new plant (140), and
319 Minato plant (89 Gg CO₂). The data for all 106 point sources are given in Table S1. The 19
320 power plants contributed 64.1% of the 2014 total point-source emissions (6,478), the 11
321 airports 18.6% (1,879), the 61 waste incineration plants 14.6% (1,483), and the 15 ports 2.8
322 % (279 Gg CO₂).

323 The highest line-source emissions for 2014 (Fig. 5) were associated with 30 road segments on
324 two urban highways: Central loop line highway in KS Ward (19.7) and the Coastline
325 highway in KT Ward (18.8 Gg CO₂ km⁻¹). The 2014 emissions from high-speed national
326 highways (total length 150 km) were 1,048 Gg CO₂ (6.4% of the total line-source emissions);
327 urban highways (576 km) 4,867 Gg CO₂ (29.8%); general national highways (726 km) 3,520
328 Gg CO₂ (21.6%); major regional roads (1,625 km) 4,761 Gg CO₂ (29.2%); and general
329 regional roads (1,614 km) 2,128 Gg CO₂ (13.0%).

330 The highest area-source emissions from the industrial and commercial sector for 2014 were
331 recorded in the inner-city areas in CD (172.4), CO (167.0), and SJ (162.0 Gg CO₂ km⁻²)
332 Wards (Fig. 6A), respectively. The industrial and commercial emissions counted from
333 economic census areas were shown in Fig. 6B. Those from the residential sector were in KT
334 (10.0), TS (9.9), and TT (9.5 Gg CO₂ km⁻²) Wards (Fig. 7A), respectively. The residential
335 emissions counted from population census areas were shown in Fig. 7B. Those from the
336 agricultural sector (Fig. 8A) were recorded in MS (0.45) and NK Cities (0.36), and EG Ward
337 (0.33 Gg CO₂ km⁻²), respectively. The agricultural emissions counted for 62 municipalities
338 (Fig. 8B) were finally allocated for high-spatial-resolution map (Fig. 8C).

339

340 **Comparison with other emission estimates**

341 The Tokyo government has reported annual GHG emissions every year since 1990, with
342 emissions being calculated with a top-down approach based on energy consumption [65]. In
343 the governmental EI, emissions for each sector in Tokyo are based on the final energy
344 consumption, including electricity, city gas, liquefied petroleum gas, and kerosene, with
345 emissions being apportioned according to economic indicators, such as family expenditure,
346 commodity values, numbers of vehicles, buildings areas, and passenger and cargo transport in
347 Tokyo.

348 Annual emissions between the present EI and the EI prepared by the Tokyo government are
349 compared for four major categories (Fig. 9A1-2). The governmental EI includes total
350 emissions from the Tokyo Metropolis of 62,120 Gg CO₂ for 2014. The governmental EI

351 includes the following emissions: 29,320 from the industrial and commercial sector; 19,650
352 from the residential sector; 11,570 from transportation; and 1,570 Gg CO₂ from waste
353 incineration. Based on the annual emissions by sector and fuel type in the report [65], we
354 derived the non-electric emissions for the residential sector from the governmental EI as
355 5,532, consistent with our result of 5,302 Gg CO₂. However, those for the industrial and
356 commercial sector are different (governmental EI 6,080, the present EI 13,085 Gg CO₂). For
357 waste incineration, the governmental EI considered only emissions from the fossil-carbon
358 content of waste (1,570), whereas we included both these emissions (1,473) and the
359 combustion agent (10 Gg CO₂).

360 The differences in emissions between the two EIs could be associated mainly with electricity
361 production. This study estimated the emissions from electricity generation as point sources
362 based on fossil-fuel consumption at power plants (direct emissions, Scope-1[6]), while the
363 Tokyo government estimated them based on the final energy consumption (consumption-
364 based emissions, Scope-2 [6]). For example, the government EI includes emissions from
365 electricity consumption by railways and the electricity generated outside the Tokyo area [66].
366 These differences resulted in higher annual emissions from electricity consumption in the
367 government EI (39,460) compared with the EI of the present study (6,478 Gg CO₂).

368 The EAGrid is a reliable EI for multiple pollutants that was developed for the East Asia
369 region in 1995 [67] and revised in 2000 with a focus on local emission sources in Japan
370 (EAGrid-Japan 2000) [68]. In the most recent version (2010), emissions were estimated by
371 adjusting the 2000 emissions according to the increase in national fuel consumption from
372 2000 to 2010 (see Fukui et al. [69]), without any change in the distribution of emission
373 sources. Here we relied on data for the Tokyo domain provided by the developer of EAGrid-
374 Japan 2010 [69].

375 Total emissions in the EAGrid-Japan 2010 EI for Tokyo are 42,009, which is 6.3% lower
376 than our estimate for 2014 (44,855 Gg CO₂). To compare the two sets of results by source
377 type, the sectoral emissions of the present EI in three categories are summarized in Fig. 9B1
378 and those for EAGrid are shown in Fig. 9B2. The point-source emissions of EAGrid (5,631
379 Gg CO₂) include those from power plants, waste incineration plants, vessels, and aircraft; line
380 sources from road transportation (14,672 Gg CO₂); and area sources (21,705 Gg CO₂) from
381 residential and commercial combustion equipment, factory and building boilers, off-road
382 transportation (construction, agricultural, and factory machine use), open burning, and
383 facilities.

384 Spatial distributions of the emissions between the two EIs were compared at a 1 × 1 km
385 resolution by scaling the total EAGrid emissions to our 2014 EI (Fig. 10). The difference in
386 the point sources (Fig. 10A) shows that some gridded emissions of this study were lower than
387 those in EAGrid. To map the gridded values of EAGrid, the counted total emissions from
388 each airport and port were allocated by the area of the facility' boundary, with the number of
389 point sources being higher than those in this study. Other differences are due to the EAGrid
390 EI, which does not include recently constructed major sources, such as Shinagawa power
391 plant and Haneda airport domestic terminal 2. As shown in Fig. 11A, the correlation of the
392 gridded emissions of point sources between the two sets of results is very low ($R^2 = 0.31$).
393 Line-source differences (Fig. 10B) vary from -100 to +100 Gg CO₂ km⁻². The differences
394 between the year of traffic census and road maps resulted in the difference in emissions. Road

395 segment lengths were obtained from the 1995 DRM in the EAGrid EI [68], whereas we used
396 the current 2015 versions. Area-source differences (Fig. 10C) are variable because the
397 EAGrid EI includes residential, industrial, commercial, off-road, open burning, and other
398 emissions as area sources, whereas this study only considers residential, industrial and
399 commercial, and agricultural sectors as area sources. The area-source emissions in the present
400 EI were 3,292 Gg CO₂, lower than those of the EAGrid. As shown in Fig. 11B-C, the
401 correlations of the gridded emissions for line and area sources between the two sets of results
402 are high ($R^2 = 0.74$ for line sources and 0.71 for area sources).
403 Differences in total emissions vary between $-1,500$ and $+4,500$ Gg CO₂ km⁻² (Fig. 10D),
404 with differences being smaller in the western mountain and forest areas and larger in the
405 inner-city areas (eastern Tokyo). As shown in Fig. 11D, the correlation of the total gridded
406 emissions between the two sets of results is moderate ($R^2 = 0.69$). The number of cells in the
407 present EI is much greater than that in EAGrid in the 0–10 Gg CO₂ km⁻² emission range (Fig.
408 12), with the present EI therefore including more low-emission areas than the EAGrid, while
409 greater 20–50 Gg CO₂ km⁻² emissions are included in the latter. The numbers of cells are
410 consistent for the other emission ranges. Thus, we could conclude that even the number of
411 cells in some emission ranges and the total annual emissions between the two sets of results
412 seem to be close but the distributions of the source emissions are different.

413

414 **Current limitations and future perspectives**

415 Uncertainties associated with emission factors, activity data, and emission spatial modeling
416 introduce uncertainties in the final emission estimates [e.g., 10, 70]. We refer to the
417 uncertainties on the basis of activity data and emission factors (Table S5) using IPCC
418 guidelines [16, 71]. The total uncertainty is estimated to be $\pm 3.57\%$, equivalent to $44,855 \pm$
419 $1,601$ Gg CO₂.

420 Uncertainties introduced from emissions calculations and mapping processes are likely to be
421 large due to the assumptions and approximations used. For example, the operation ratio of
422 power plants varies with individual plants; however, this study applied averaged operating
423 ratios for the whole plants in the calculation process. This approach reduces the variability in
424 emissions at each power plant, leading to poor representation of emissions with higher
425 temporospatial resolution than we applied here. The road segments that are not fully covered
426 by the census contribute over 4,205 km in our calculation. We substituted the average traffic
427 conditions for the road segments to estimate the emissions. This approach could overestimate
428 the traffic quantities and emissions for the segments.

429 In mapping processes, this study treated the mobile emissions of aircraft and vessels as point
430 sources. This means that the whole emissions over their moving paths were aggregated to a
431 point, leading to an overestimate of the point-source emissions. The building emissions were
432 estimated using TFAs of buildings in each census area. In this estimate we used DSM data
433 with a spatial resolution of 30 m, but this spatial resolution is insufficient to calculate the
434 heights and TFAs for individual buildings. Additionally, our downscale approach did not
435 distinguish occupied and vacant houses. All of these limitations should be improved in the
436 next study. As in previous studies (e.g., Hestia [14]), better data availability for emissions
437 calculations and mapping should greatly improve the accuracy of estimates.

438 We plan to update our emission estimates once updated activity data become available. The
439 methods employed here are applicable to other parts of Japan, and the entire country could be
440 covered, although further objective evaluation is necessary. Future work should also include
441 improvements of the methodology for mapping emissions from traffic on narrow roads,
442 modeling of temporal variations (seasonal, weekly, and diurnal), and extending the time
443 period of this study.

444

445 **Conclusions**

446 Spatially explicit estimates of FFCO₂ emissions were prepared for the Tokyo Metropolis,
447 with the EI being primarily compiled using a bottom-up approach. Following the 2006 IPCC
448 guidelines, geolocation data were collected for point, line, and area sources, with the
449 emissions mapped where possible. Detailed activity data, including the operating ratios of
450 power plants, load factors of vessels, fossil-carbon contents of waste, and emission factors for
451 fossil-fueled power generation, aircraft movements, navigation, and combustion processes,
452 were utilized to improve the accuracy of emission estimates. The utilization of spatially
453 verified national census data, regional/city specific emission factors, and emission factors for
454 road segments, as well as the consideration of low-emission sectors, such as waterborne
455 navigation and agricultural machinery use, were highlighted. This EI demonstrated that the
456 Tier 3 approach could be applicable not only at a national scale but also a sub-national scale.
457 The total emissions from the Tokyo Metropolis in 2014 were estimated to be 44,855 Gg CO₂.
458 The highest emission sector was road transportation (16,323 Gg CO₂), which accounted for
459 36.4% of the total emissions. Spatial emission patterns were compared with those of EAGrid-
460 Japan, highlighting differences in the distributions of source types. The differences resulted
461 mainly from the counting and mapping approaches used, and the different sector categories.
462 This methodology is applicable to other prefectures and can be used to cover the entire
463 country. This EI facilitates the acquisition of information on emissions from high-emission
464 point sources, buildings, and road segments more than other gridded datasets. It may also be
465 used to validate other EIs and to prepare urban carbon budgets in addition to aiding policy
466 makers in controlling GHG emissions.

467

468 **Abbreviations**

469 CO₂: carbon dioxide

470 FFCO₂: carbon dioxide emissions from fossil fuel combustion

471 EI: emission inventory

472 GPC: Global Protocol for Community-Scale Greenhouse Gas Emission Inventories

473 UNFCCC: UN Framework Convention on Climate Change

474 IPCC: Intergovernmental Panel on Climate Change

475 GHG: greenhouse gas

476 GESAPU: National geoinformation technologies, spatiotemporal approaches, and the
477 Protocol for Reducing GHG Emission Uncertainties
478 EAGrid-Japan: East Asian Air Pollutant Emission Grid Database for Japan
479 MW: megawatt
480 LTO: landing and take-off
481 ICAO: International Civil Aviation Organization
482 GT: gross tonnage
483 MSW: municipal solid waste
484 CA: combustion agent
485 DRM: digital road map
486 GIS: geographic information system
487 TFA: total floor area
488 DSM: digital surface model
489 DEM: digital elevation model

490

491 **Declarations**

492 **Ethics approval and consent to participate**

493 Not applicable.

494 **Consent for publication**

495 Not applicable.

496 **Availability of data and materials**

497 The data used in this study are either presented in this manuscript or available from the data
498 sourced indicated. The authors plan to make the data product developed in this study publicly
499 available with a DOI.

500 **Competing interests**

501 The authors declare that they have no competing interests.

502 **Funding**

503 This study was funded by the Ministry of the Environment, Japan, and partly supported by
504 the Low-Carbon Research Program of the National Institute for Environmental Studies.

505 **Authors' contributions**

506 RC carried out the data collection and analysis with support from MS. TF provided the EAGrid-
507 Japan2010 emission inventory and guidance on the use of the inventory in the data analysis.
508 RC wrote the manuscript with input from MS. RC and AI provided critical comments and
509 shaped the study and manuscript. All the authors contributed to the final version of the
510 manuscript and approved the submission.

511 **Acknowledgements**

512 We thank Tomohiro Oda who conceived this study, and provided valuable input and feedback
513 to the data analysis as well as manuscript development. The authors also acknowledge that this
514 study greatly benefited from the Master's thesis work done by Yutaka Mori at Osaka University
515 under the supervision of Tomohiro Oda. We thank Shamil Maksyutov from the National
516 Institute for Environment Studies for his valuable comments on this article.

517 **Authors' information**

518 **Affiliations**

519 Center for Global Environmental Research, National Institute for Environmental Studies, 16-
520 2, Onogawa, Tsukuba, Ibaraki, 305-8506, Japan

521 Richao Cong, Makoto Saito, Ryuichi Hirata & Akihiko Ito

522 Fukushima Branch, National Institute for Environmental Studies, Fukushima Environmental
523 Creation Centre, 10-2, Fukasaku, Miharu Town, Tamura District, Fukushima, 963-7700, Japan

524 Richao Cong

525 Institute of Behavioral Sciences, 2-9, Ichigaya-honmuracho, Shinjuku-ku, Tokyo, 162-0845,
526 Japan

527 Tetsuo Fukui

528 **Corresponding authors**

529 Correspondence to Richao Cong or Makoto Saito.

530

531 **References**

- 532 1. Le Quéré C, Andrew RM, Friedlingstein P, Sitch S, Pongratz J, Manning AC, et al.
533 Global Carbon Budget 2017. *Earth Syst Sci Data*. 2018;10:405-48.
534 <https://doi.org/10.5194/essd-10-2141-2018>.
- 535 2. UN-Habitat. The challenge. <https://unhabitat.org/topic/climate-change>. Accessed 1 Jan
536 2020.
- 537 3. Hoornweg D, Sugar L, Gómez CLT. Cities and greenhouse gas emissions: moving
538 forward. *Environ Urban*. 2011;23:207–27.
- 539 4. C40 Cities Climate Leadership Group. <https://www.c40.org/>. Accessed 1 Jan 2020.
- 540 5. Global Covenant of Mayors for Climate & Energy.
541 <https://www.globalcovenantofmayors.org/>. Accessed 1 Jan 2020.
- 542 6. Fong WK, Sotos M, Michael Doust M, Schultz S, Marques A, Deng-Beck C, et al.
543 Global Protocol for Community-Scale Greenhouse Gas Emission Inventories. 2015.
544 <http://ghgprotocol.org/greenhouse-gas-protocol-accounting-reporting-standard-cities>.
545 Accessed 1 Jan 2020.
- 546 7. United Nations. Paris Agreement. 2015. [https://unfccc.int/process-and-meetings/the-](https://unfccc.int/process-and-meetings/the-paris-agreement/what-is-the-paris-agreement)
547 [paris-agreement/what-is-the-paris-agreement](https://unfccc.int/process-and-meetings/the-paris-agreement/what-is-the-paris-agreement). Accessed 1 Jan 2020.
- 548 8. United Nations. Kyoto Protocol to the United Nations Framework Convention on
549 Climate Change. 1998. [https://unfccc.int/process-and-meetings/the-kyoto-protocol/what-](https://unfccc.int/process-and-meetings/the-kyoto-protocol/what-is-the-kyoto-protocol/what-is-the-kyoto-protocol)
550 [is-the-kyoto-protocol/what-is-the-kyoto-protocol](https://unfccc.int/process-and-meetings/the-kyoto-protocol/what-is-the-kyoto-protocol/what-is-the-kyoto-protocol). Accessed 1 Jan 2020.
- 551 9. Gurney KR, Liang J, O’Keeffe D, Patarasuk R, Hutchins M, Huang J, et al. Comparison
552 of Global Downscaled Versus Bottom-Up Fossil Fuel CO₂ Emissions at the Urban Scale
553 in Four US Urban Areas. *J Geophys Res Atmos*. 2019;124:2823-40.
554 <https://doi.org/10.1029/2018JD028859>.
- 555 10. Bun R, Nahorski Z, Horabik-Pyzel J, Danylo O, See L, Charkovska N, et al.
556 Development of a high-resolution spatial inventory of greenhouse gas emissions for
557 Poland from stationary and mobile sources. *Mitig Adapt Strateg Glob Chang*. 2018.
558 <https://doi.org/10.1007/s11027-018-9791-2>.
- 559 11. Gurney KR, Razlivanov I, Song Y, Zhou Y, Benes B, Abdul-Massih M. Quantification
560 of fossil fuel CO₂ emissions on the building/street scale for a large US city. *Environ Sci*
561 *Technol*. 2012. <http://doi.org/10.1021/es3011282>.
- 562 12. Gurney KR, Patarasuk P, Liang J, Song Y, O’Keeffe D, Rao P, et al. The Hestia fossil
563 fuel CO₂ emissions data product for the Los Angeles megacity (Hestia-LA), *Earth Syst*.
564 *Sci. Data*. 2019. <https://doi.org/10.5194/essd-11-1309-2019>.

- 565 13. Patarasuk P, Gurney KR, O’Keeffe D, Song Y, Huang J, Rao P, et al. Urban high-
566 resolution fossil fuel CO₂ emissions quantification and exploration of emission drivers
567 for potential policy applications. Urban Ecosyst. 2016. [https://doi.org/10.1007/s11252-](https://doi.org/10.1007/s11252-016-0553-1)
568 [016-0553-1](https://doi.org/10.1007/s11252-016-0553-1).
- 569 14. The Hestia Project. http://hestia.project.asu.edu/audience_researchers.shtml. Accessed 1
570 Jan 2020.
- 571 15. Mori Y. Development of high spatial- and temporal- resolution anthropogenic CO₂
572 inventory in Osaka Prefecture (Master thesis). 2016. [http://www.see.eng.osaka-](http://www.see.eng.osaka-u.ac.jp/seege/seege/material/2016/mori.pdf)
573 [u.ac.jp/seege/seege/material/2016/mori.pdf](http://www.see.eng.osaka-u.ac.jp/seege/seege/material/2016/mori.pdf). Accessed 1 Jan 2020.
- 574 16. IPCC. 2006 IPCC Guidelines for National Greenhouse Gas Inventories. 2007.
575 <https://www.ipcc-nggip.iges.or.jp/public/2006gl/>. Accessed 1 Jan 2020.
- 576 17. Electrical Japan. Fossil fuel fired power generation information. 2017.
577 [http://agora.ex.nii.ac.jp/earthquake/201103-eastjapan/energy/electrical-](http://agora.ex.nii.ac.jp/earthquake/201103-eastjapan/energy/electrical-japan/area/13.html.ja)
578 [japan/area/13.html.ja](http://agora.ex.nii.ac.jp/earthquake/201103-eastjapan/energy/electrical-japan/area/13.html.ja). Accessed 1 Jan 2020. **(in Japanese)**
- 579 18. Tokyo Gas Engineering Solutions. The list of plants built under the redevelopment.
580 <http://www.tokyogas-es.co.jp/case/#anchor08>. Accessed 1 Jan 2020. **(in Japanese)**
- 581 19. Tokyo electric power company holdings. The list of power plants: steam and internal
582 combustion types. [http://www.tepco.co.jp/corporateinfo/illustrated/electricity-](http://www.tepco.co.jp/corporateinfo/illustrated/electricity-supply/index-j.html)
583 [supply/index-j.html](http://www.tepco.co.jp/corporateinfo/illustrated/electricity-supply/index-j.html). Accessed 1 Jan 2020. **(in Japanese)**
- 584 20. Mori building. The introduction for Roppongi energy service plant.
585 <https://www.mori.co.jp/morinow/2011/05/2011051216000002184.html>. Accessed 1 Jan
586 2020. **(in Japanese)**
- 587 21. Agency for Natural Resources and Energy. Running ratio of fossil-fueled power plants in
588 2014. 2015. [https://www.enecho.meti.go.jp/statistics/electric_power/ep002/xls/2014/2-4-](https://www.enecho.meti.go.jp/statistics/electric_power/ep002/xls/2014/2-4-H26.xls)
589 [H26.xls](https://www.enecho.meti.go.jp/statistics/electric_power/ep002/xls/2014/2-4-H26.xls). Accessed 1 Jan 2020. **(in Japanese)**
- 590 22. Agency for Natural Resources and Energy. Energy consumption and electricity
591 generation amount by power plants. 2014.
592 https://www.enecho.meti.go.jp/statistics/electric_power/ep002/xls/2014/4-1-H26.xls.
593 https://www.enecho.meti.go.jp/statistics/electric_power/ep002/xls/2014/4-2-H26.xls.
594 https://www.enecho.meti.go.jp/statistics/electric_power/ep002/xls/2014/4-3-H26.xls.
595 Accessed 1 Jan 2020. **(in Japanese)**
- 596 23. Ministry of the Environment. Guidelines for Calculation Method on Greenhouse Gas
597 Emissions. 2017. https://ghg-santeikohyo.env.go.jp/files/manual/chpt2_4-4.pdf.
598 Accessed 1 Jan 2020. **(in Japanese)**
- 599 24. Ministry of Land, Infrastructure, Transport and Tourism. Annual record of airport
600 management. 2015. <http://www.mlit.go.jp/common/001296737.xls>. Accessed 1 Jan
601 2020. **(in Japanese)**
- 602 25. Toho Air Service. Safety report for 2015: the types of helicopters.
603 <http://www.tohoair.co.jp/english/index.html>. Accessed 1 Jan 2020. **(in Japanese)**
- 604 26. New Central Airservice. Safety report for 2015: the types of aircrafts.
605 <https://www.central-air.co.jp/en/index.html>. Accessed 1 Jan 2020. **(in Japanese)**
- 606 27. Air Do. Safety report for 2015. <https://www.airdo.jp/en/>. Accessed 1 Jan 2020. **(in**
607 **Japanese)**

- 608 28. All Nippon Airways. ANA group safety report for 2015. <https://www.ana.co.jp/en/jp/>.
609 Accessed 1 Jan 2020. **(in Japanese)**
- 610 29. Japan Airlines. JAL safety report for 2015. <http://www.jal.com/en/>. Accessed 1 Jan 2020.
611 **(in Japanese)**
- 612 30. Skymark Airlines. Safety report for 2015. <https://www.skymark.jp/en/>. Accessed 1 Jan
613 2020. **(in Japanese)**
- 614 31. Solaseed Air. Safety report for 2015. <https://www.solaseedair.jp/en/>. Accessed 1 Jan
615 2020. **(in Japanese)**
- 616 32. Starflyer. Safety report for 2015. <https://www.starflyer.jp/en/>. Accessed 1 Jan 2020. **(in**
617 **Japanese)**
- 618 33. Flugzeuginfo.net. Aircraft types. 2017. http://www.flugzeuginfo.net/acdata_en.php.
619 Accessed 1 Jan 2020.
- 620 34. Haneda Airport International Passenger Terminal. Domestic flight information. 2017.
621 <http://www.tokyo-airport-bldg.co.jp/en/flight/>. Accessed 1 Jan 2020.
- 622 35. Haneda Airport International Passenger Terminal. International flight information. 2017.
623 <http://www.haneda-airport.jp/inter/flight/showFlightScheduleSearch?langId=en>.
624 Accessed 1 Jan 2020.
- 625 36. European Union Aviation Safety Agency. ICAO Aircraft Engine Emissions Databank.
626 2017. [https://www.easa.europa.eu/sites/default/files/dfu/edb-emissions-](https://www.easa.europa.eu/sites/default/files/dfu/edb-emissions-databank%20v26B-NewFormat%20%28web%29.xlsx)
627 [databank%20v26B-NewFormat%20%28web%29.xlsx](https://www.easa.europa.eu/sites/default/files/dfu/edb-emissions-databank%20v26B-NewFormat%20%28web%29.xlsx). Accessed 1 Jan 2020.
- 628 37. Federal Office of Civil Aviation. Guidance on the Determination of Helicopter
629 Emissions. 2013.
630 [https://www.bazl.admin.ch/dam/bazl/de/dokumente/Fachleute/Regulationen_und_Grundl](https://www.bazl.admin.ch/dam/bazl/de/dokumente/Fachleute/Regulationen_und_Grundlagen/guidance_on_the_determinationofhelicopteremissions.pdf.download.pdf/guidance_on_the_determinationofhelicopteremissions.pdf)
631 [agen/guidance_on_the_determinationofhelicopteremissions.pdf.download.pdf/guidance](https://www.bazl.admin.ch/dam/bazl/de/dokumente/Fachleute/Regulationen_und_Grundlagen/guidance_on_the_determinationofhelicopteremissions.pdf.download.pdf/guidance_on_the_determinationofhelicopteremissions.pdf)
632 [on_the_determinationofhelicopteremissions.pdf](https://www.bazl.admin.ch/dam/bazl/de/dokumente/Fachleute/Regulationen_und_Grundlagen/guidance_on_the_determinationofhelicopteremissions.pdf.download.pdf/guidance_on_the_determinationofhelicopteremissions.pdf). Accessed 1 Jan 2020.
- 633 38. Ministry of the Environment. The emissions from ships. 2011.
634 <https://www.google.com/url?sa=t&rct=j&q=&esrc=s&source=web&cd=5&ved=2ahUK>
635 [EwjTnbqFkpvAhXULqYKHWviAr8QFjAEegQIAxAB&url=https%3A%2F%2Fwww.](https://www.google.com/url?sa=t&rct=j&q=&esrc=s&source=web&cd=5&ved=2ahUK)
636 [env.go.jp%2Fchemi%2Fprtr%2Fresult%2FtodokedegaiH24%2Fsyosai%2F14.pdf&usg=](https://www.google.com/url?sa=t&rct=j&q=&esrc=s&source=web&cd=5&ved=2ahUK)
637 [AOvVaw1k0HFRRuhNLhaq87xHZuYb](https://www.google.com/url?sa=t&rct=j&q=&esrc=s&source=web&cd=5&ved=2ahUK). Accessed 1 Jan 2020. **(in Japanese)**
- 638 39. OPRI. Investigation report on the environmental impact of PM by vessels. 2007.
639 <http://fields.canpan.info/report/download?id=3269>. Accessed 1 Jan 2020. **(in Japanese)**
- 640 40. Ministry of Land, Infrastructure, Transport and Tourism. Annual report on vessels at
641 Tokyo port. <https://www.mlit.go.jp/common/001277697.xls>. Accessed 1 Jan 2020. **(in**
642 **Japanese)**
- 643 41. Bureau of Port and Harbor. Annual report on vessels on ports from the islands.
644 https://www.kouwan.metro.tokyo.lg.jp/yakuwari/27kousei_7_2.xls. Accessed 1 Jan
645 2020. **(in Japanese)**
- 646 42. Clean Authority of Tokyo. Waste disposal of Tokyo 23cities: Annual report on the waste
647 incineration plants of Tokyo in 2014. 2016. [https://www.union.tokyo23-](https://www.union.tokyo23-seisou.lg.jp/gijutsu/gijutsu/kumiai/shiryo/documents/26honbun.pdf)
648 [seisou.lg.jp/gijutsu/gijutsu/kumiai/shiryo/documents/26honbun.pdf](https://www.union.tokyo23-seisou.lg.jp/gijutsu/gijutsu/kumiai/shiryo/documents/26honbun.pdf). Accessed 1 Jan
649 2020. **(in Japanese)**
- 650 43. Ministry of the Environment. Investigation result on the municipal solid waste disposal
651 status of Tokyo in 2014. 2017.

- 652 http://www.env.go.jp/recycle/waste_tech/ippan/h26/data/seibi/city/13.xlsx. Accessed 1
653 Jan 2020. **(in Japanese)**
- 654 44. Bureau of Environment Tokyo Metropolitan Government. Investigation Report on the
655 Status of Industrial Waste of Tokyo in 2014. 2016.
656 https://www.kankyo.metro.tokyo.lg.jp/resource/industrial_waste/notification/investigation.files/H26houkokusyo.pdf. Accessed 1 Jan 2020. **(in Japanese)**
- 657
658 45. Bureau of Environment Tokyo Metropolitan Government. Waste disposal facilities in
659 Tokyo. 2017.
660 https://www.kankyo.metro.tokyo.lg.jp/resource/general_waste/processing_plant/processing_plant.files/20200101_shisetsulist.pdf. Accessed 1 Jan 2020. **(in Japanese)**
- 661
662 46. Ministry of Land, Infrastructure, Transport and Tourism. Traffic Census. 2015.
663 <http://www.mlit.go.jp/road/census/h27/data/xlsx/kasyo13.xlsx>. Accessed 1 Jan 2020. **(in**
664 **Japanese)**
- 665 47. Japan Digital Road Map Association. Digital road map. 2017.
666 <https://www.drm.jp/english/>. Accessed 1 Jan 2020.
- 667 48. Ministry of Land, Infrastructure, Transport and Tourism. National Land Numerical
668 Information Download Service: Administrative zones data. 2014.
669 http://nlftp.mlit.go.jp/ksj-e/gml/datalist/KsjTmplt-N03-v2_3.html. Accessed 1 Jun 2019.
- 670 49. Dohi M, Shinri S, Masamichi T. Renewal of the Emission Factor of Carbon Dioxide and
671 Fuel Consumption for Motor Vehicles. Technical note of NILIM. 2012;54:40-5.
672 www.pwrc.or.jp/thesis_shouroku/thesis_pdf/1204-P040-045_dohi.pdf. Accessed 1 Jan
673 2020. **(in Japanese)**
- 674 50. United States Department of Energy. eQUEST. 2009. <http://doe2.com/equest/index.html>.
675 Accessed 1 Jan 2020.
- 676 51. Zhou Y, Gurney K. A new methodology for quantifying on-site residential and
677 commercial fossil fuel CO₂ emissions at the building spatial scale and hourly time scale.
678 Carbon Manag. 2010;1:45-56.
- 679 52. Statistics Japan. 2014 Economic Census. 2016. [http://www.stat.go.jp/english/data/e-](http://www.stat.go.jp/english/data/e-census/index.html)
680 [census/index.html](http://www.stat.go.jp/english/data/e-census/index.html). Accessed 1 Jan 2020.
- 681 53. Agency for Natural Resources and Energy. Energy-balance table of Tokyo. 2017.
682 https://www.enecho.meti.go.jp/statistics/energy_consumption/ec002/xls/13tokyo.xls.
683 Accessed 1 Jan 2020. **(in Japanese)**
- 684 54. Gately CK, Hutyra LR. Large Uncertainties in Urban-Scale Carbon Emissions. J
685 Geophys Res Atmos. 2017;122:242-60.
- 686 55. Bureau of Urban Development Tokyo Metropolitan Government. Land use of Tokyo.
687 2014. https://www.toshiseibi.metro.tokyo.lg.jp/seisaku/tochi_c/pdf/tochi_5/tochi_all.pdf.
688 Accessed 1 Jan 2020. **(in Japanese)**
- 689 56. Japan Aerospace Exploration Agency. ALOS Global Digital Surface model (AW3D30).
690 2015. <https://www.eorc.jaxa.jp/ALOS/en/aw3d30/data/index.htm>. Accessed 1 Jan 2020.
- 691 57. Geospatial Information Authority of Japan, Building polygons and digital elevation
692 model. 2017. <https://fgd.gsi.go.jp/download/menu.php>. Accessed 1 Jan 2020. **(in**
693 **Japanese)**
- 694 58. Statistics Japan. 2015 Population Census. 2017.
695 <http://www.stat.go.jp/english/data/kokusei/index.html>. Accessed 1 Jan 2020.

- 696 59. Statistics Japan. Investigation in 2014-2015 for counting the CO₂ emissions from
697 households. 2016. <https://www.e-stat.go.jp/en>. Accessed 1 Jan 2020. **(in Japanese)**
- 698 60. Statistics of Tokyo. Investigation result on Agricultural census in Tokyo 2015. 2017.
699 <https://www.toukei.metro.tokyo.lg.jp/nourin/2015/ng15ta1400.xls>. Accessed 1 Jan 2020.
700 **(in Japanese)**
- 701 61. Tokyo Development Foundation for Agriculture, Forestry, and Fisheries. Investigation
702 on the condition of agricultural products in Tokyo 2014. 2016.
703 https://tokyogrown.jp/learning/library/img/agriculture_report_2014.pdf. Accessed 1 Jan
704 2020. **(in Japanese)**
- 705 62. National Institute for Agro-Environmental Sciences. Life Cycle Assessment for
706 Environmentally Sustainable Agriculture. NIAES Report. 2003.
707 http://www.naro.affrc.go.jp/archive/niaes/project/lca/lca_r.pdf. Accessed 1 Jun 2019. **(in**
708 **Japanese)**
- 709 63. Shimizu N, Yuyama Y. Analysis of the energy consumption and profitability of
710 agricultural practice with environmental consciousness-a case study in north-eastern
711 Chiba Prefecture. J Rural Plan Assoc. 2007;26:365-70. **(abstract in English and text in**
712 **Japanese)**[https://www.jstage.jst.go.jp/article/arp/26/Special_Issue/26_Special_Issue_36](https://www.jstage.jst.go.jp/article/arp/26/Special_Issue/26_Special_Issue_365/article-char/en)
713 [5/ article-char/en](https://www.jstage.jst.go.jp/article/arp/26/Special_Issue/26_Special_Issue_365/article-char/en). Accessed 1 Jan 2020.
- 714 64. Japan Aerospace Exploration Agency. Homepage of High-resolution Land Use and Land
715 Cover Map Products: HRLULC 10m resolution map of Japan [2006-2011] (ver.16.09).
716 2016. http://www.eorc.jaxa.jp/ALOS/en/lulc/lulc_index.htm. Accessed 1 Jan 2020.
- 717 65. Bureau of Environment Tokyo Metropolitan Government. Final Energy Consumption
718 and Greenhouse Gas Emissions in Tokyo (FY 2014). 2017.
719 [https://www.kankyo.metro.tokyo.lg.jp/en/climate/index.files/b0548c2a69e7883f1945aca](https://www.kankyo.metro.tokyo.lg.jp/en/climate/index.files/b0548c2a69e7883f1945aca50f606a92.pdf)
720 [50f606a92.pdf](https://www.kankyo.metro.tokyo.lg.jp/en/climate/index.files/b0548c2a69e7883f1945aca50f606a92.pdf). Accessed 1 Jan 2020.
- 721 66. Agency for Natural Resources and Energy. Actual conditions on power generation and
722 transmission. 2017.
723 https://www.enecho.meti.go.jp/statistics/electric_power/ep002/xls/2014/2-5-H26.xls.
724 Accessed 1 Jan 2020. **(in Japanese)**
- 725 67. Tonooka Y, Kannari A, Higashino H, Murano K. NMVOCs and CO emission inventory
726 in East Asia. Water Air and Soil Pollut. 2001;130:199-204.
- 727 68. Kannari A, Tonooka Y, Baba T, Murano K. Development of multiple-species 1km× 1km
728 resolution hourly basis emissions inventory for Japan. Atmos Environ. 2007.
729 <https://doi.org/10.1016/j.atmosenv.2006.12.015>.
- 730 69. Fukui T, Kokuryo K, Baba T, Kannari A. Updating EAGrid2000-Japan emissions
731 inventory based on the recent emission trends. J Jpn Soc Atmos Environ. 2014;49:117-
732 25. [https://www.jstage.jst.go.jp/article/taiki/49/2/49_117/ article](https://www.jstage.jst.go.jp/article/taiki/49/2/49_117/article). Accessed 1 Jan 2020.
733 **(abstract in English and text in Japanese)**
- 734 70. Hogue S, Marland E, Andres RJ, Marland G, Woodard D. Uncertainty in gridded CO₂
735 emissions estimates. Earth' Future. 2016;4:225-39.
736 <https://doi.org/10.1002/2015EF000343>.
- 737 71. IPCC. Good Practice Guidance and Uncertainty Management in National Greenhouse
738 Gas inventories. 2000. <https://www.ipcc-nggip.iges.or.jp/public/gp/english/>. Accessed 1
739 Jan 2020.

740
741
742
743
744
745
746
747
748
749
750
751
752
753
754
755
756
757
758
759
760
761
762
763
764
765
766
767
768
769
770
771
772
773
774
775
776
777
778
779
780
781
782
783

Figure captions

Fig. 1. Conceptual framework for emission mapping.

Fig. 2. Examples of vector maps for emission sources in SG Ward, Tokyo. (A) Locations of point emission sources. (B) Road segments for line sources. (C) Building polygons for area sources (blue line shows the boundary of the area). (D) 3D emission map for all sources (Gg CO₂ yr⁻¹ per road segment for road emissions and Gg CO₂ yr⁻¹ per polygon for others).

Fig. 3. Emission maps with 1 × 1 km mesh for (A) point sources, (B) line sources, (C) area sources, and (D) all sources. Unit: Gg CO₂ km⁻² yr⁻¹.

Fig. 4. Map of 106 point sources in Tokyo (areas in blue frames indicate islands). The point in cyan indicates the highest emissions at Shinagawa power plant (3,219 Gg CO₂ yr⁻¹).

Fig. 5. Map of emissions from line sources for each road segment. The 30 road segments with the highest emissions are marked in black. Unit: Gg CO₂ km⁻¹ yr⁻¹.

Fig. 6. Map of emissions from the industrial and commercial sector with (A) 1 × 1 km mesh, unit: Gg CO₂ km⁻² yr⁻¹; (B) 5,318 economic census areas, unit: Gg CO₂ yr⁻¹. The municipality boundary for the area with the highest annual emissions (up to 82.2 Gg CO₂) is marked in cyan.

Fig. 7. Map of emissions from the residential sector with (A) 1 × 1 km mesh, unit: Gg CO₂ km⁻² yr⁻¹; (B) 5,578 population census areas, unit: Gg CO₂ yr⁻¹. The municipality boundary for the area with the highest annual emissions (up to 6.6 Gg CO₂) is marked in cyan.

Fig. 8. Maps of emissions from the agricultural machine use sector with (A) 1 × 1 km mesh, unit: Mg CO₂ km⁻² yr⁻¹. (B) 62 municipalities, unit: Mg CO₂ yr⁻¹. The area with the highest annual emissions (2,765 Mg CO₂ yr⁻¹) is marked in cyan. (C) high-spatial-resolution map on a grid with cell size of 10 × 10 m, unit: Kg CO₂ yr⁻¹ per cell.

Fig. 9. Comparisons on annual CO₂ emissions in Tokyo between the present EI (A-1) and Tokyo government 2014 EI (A-2), and between the present EI (B-1) and EAGrid-Japan 2010 (B-2). Unit: Gg CO₂.

Note: In A-1, the industrial and commercial category includes emissions from the industrial and commercial sector and the electricity generation sector. The transportation category includes emissions from the road transportation, civil aviation, and waterborne navigation sectors.

In A-2, the transportation category includes emissions from the railway, road transportation, civil aviation, and waterborne navigation sectors.

In B-2, point sources include power plants, waste incineration plants, vessels, and aircrafts. Line sources refer to road transportation. Area sources include residential and commercial combustion equipment, factory and building boilers, off-road transportation, open burning, and facilities without identified locations.

784 **Fig. 10.** Differences in emissions between the present EI and 2010 EAGrid-Japan EI at a
785 resolution of 1×1 km for: (A) point sources, (B) line sources, (C) area sources, and (D) all
786 sources. Unit: $\text{Gg CO}_2 \text{ km}^{-2} \text{ yr}^{-1}$. (Difference = emissions from the present EI – 2010
787 EAGrid-Japan EI, after adjustment of EAGrid emissions, as described in the text.).
788

789 **Fig. 11.** Scatter plots of gridded emissions by source types between the present EI and
790 EAGrid for: (A) point sources, (B) line sources, (C) area sources, and (D) all sources. Unit:
791 $\log_{10} \text{Gg CO}_2 \text{ km}^{-2} \text{ yr}^{-1}$.
792

793 **Fig. 12.** Frequency distribution of gridded emissions ($\text{Gg CO}_2 \text{ km}^{-2} \text{ yr}^{-1}$) for this study
794 (green) and EAGrid-Japan 2010 adjusted (blue). $n = 2,688$.
795

796 **Table captions**

797 **Table 1** Spatial data used for identifying CO₂ emission sources, and other data used for
798 counting emissions for each sector in Tokyo. Note that several sectors are not consistent with
799 the IPCC definitions. For example, (1) only the LTO cycle emissions were used here for civil
800 aviation, whereas the IPCC sector includes emissions from LTO cycle and cruise; (2) only
801 passenger and cargo ships with round trips to the ports were considered here for the
802 waterborne navigation sector, whereas the IPCC sector covers all water-borne transport, from
803 recreational craft to large ocean-going cargo ships; and (3) two IPCC sectors (manufacturing
804 and commercial sectors) were combined to form the industrial and commercial sector.
805

806 **Table 2** CO₂ emission factors for vehicles by vehicle type and speed (2010), extracted from
807 experimental results [49].
808

809 **Table 3** Annual consumption of fossil fuels, worker numbers, and CO₂ emission factors for
810 workers by category in Tokyo, derived from the 2014 economic census [52] and the energy-
811 balance table for Tokyo (2014) [53].
812

813 **Table 4** CO₂ emission factors for households by occupancy and building type, based on an
814 investigation of residential energy consumption [59].
815

816 **Table 5** CO₂ emission factors for farmland by crop type [62, 63].
817

818 **Table 6** Estimates of annual CO₂ emissions from Tokyo (2014) by sector and source type.
819

820 **Additional file 1**

821 **Table S1** Ownership, facility description, location, and emissions for 106 point-type emission
822 sources (2014). Note: * indicates that the average utilization rate of CAs (2014) from these facilities
823 was extended to all of the waste incineration plants.

- 824 **Table S2** Municipality names, abbreviations, areas, populations, and emissions for the 62
825 Tokyo municipalities (2014).
- 826 **Table S3** Parameter setting for calculation the emissions from vessels [38, 39].
- 827 **Table S4** Components of this study and relevant data sources.
- 828 **Table S5** Uncertainties from activity data and emission factors, by sector.

Figures

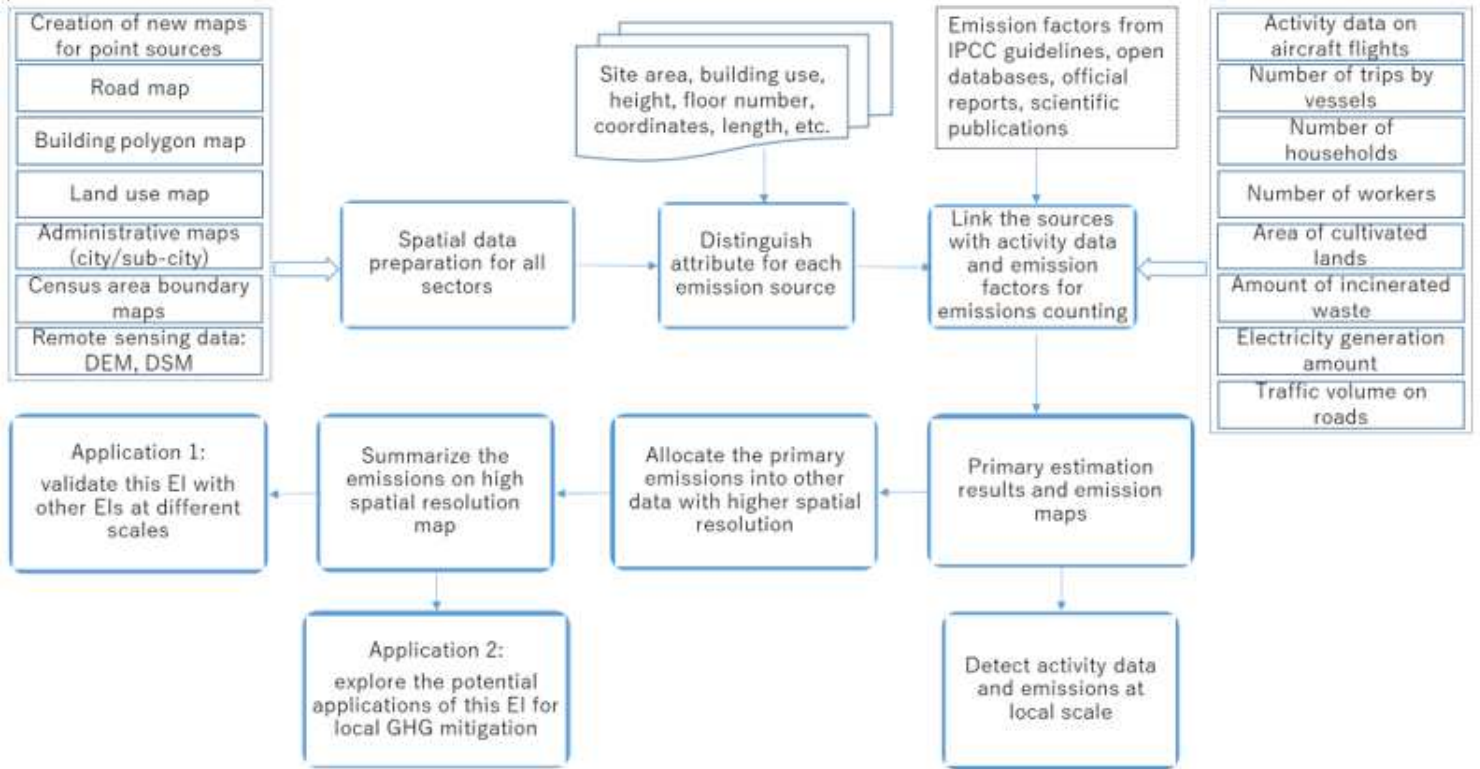


Figure 1

Conceptual framework for emission mapping.

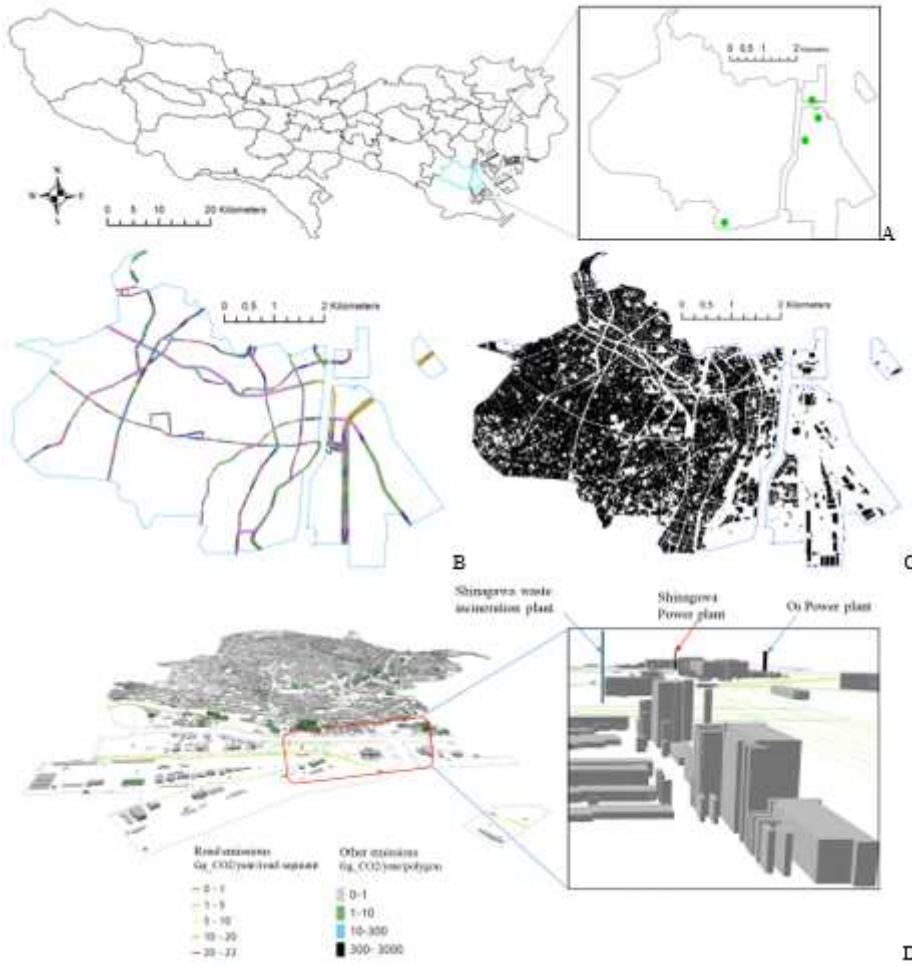


Figure 2

Examples of vector maps for emission sources in SG Ward, Tokyo. (A) Locations of point emission sources. (B) Road segments for line sources. (C) Building polygons for area sources (blue line shows the boundary of the area). (D) 3D emission map for all sources (Gg CO₂ yr⁻¹ per road segment for road emissions and Gg CO₂ yr⁻¹ per polygon for others).

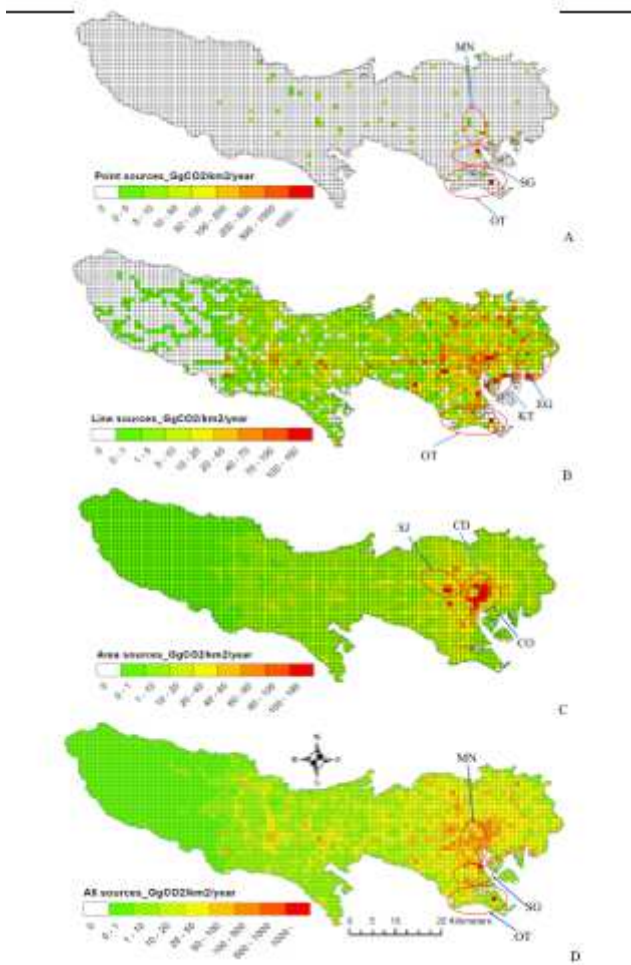


Figure 3

Emission maps with 1×1 km mesh for (A) point sources, (B) line sources, (C) area sources, and (D) all sources. Unit: Gg CO₂ km⁻² yr⁻¹.

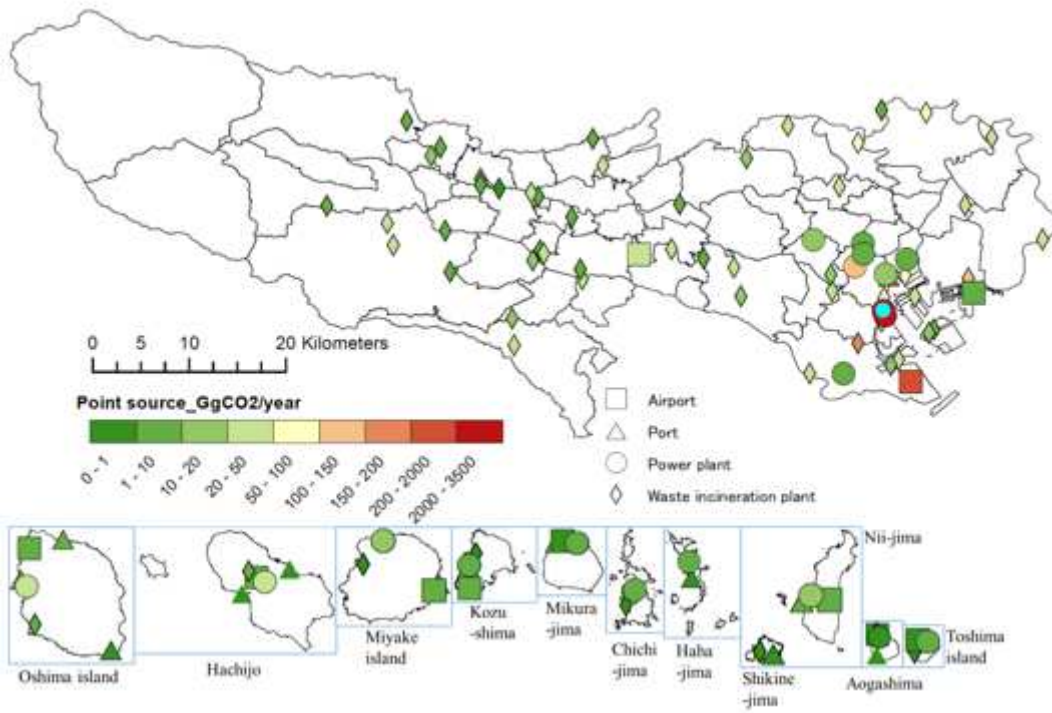


Figure 4

Map of 106 point sources in Tokyo (areas in blue frames indicate islands). The point in cyan indicates the highest emissions at Shinagawa power plant (3,219 Gg CO₂ yr⁻¹).

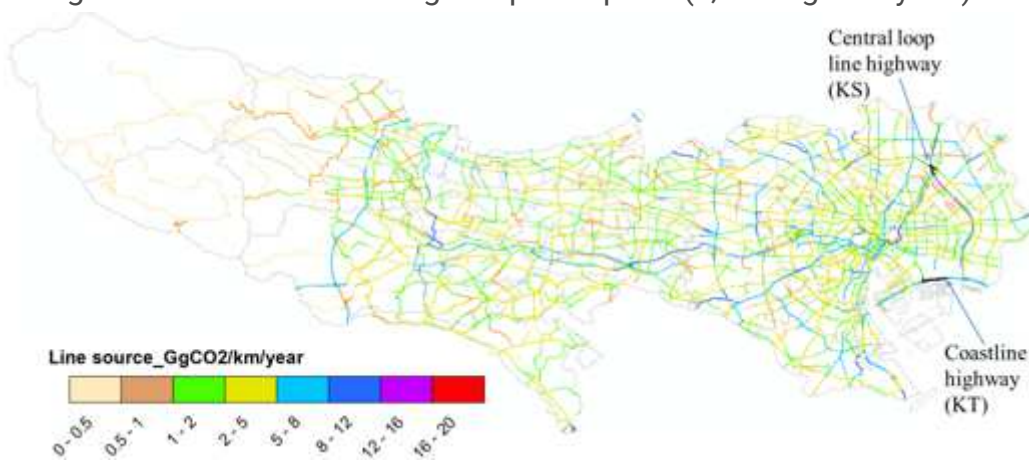


Figure 5

Map of emissions from line sources for each road segment. The 30 road segments with the highest emissions are marked in black. Unit: Gg CO₂ km⁻¹ yr⁻¹.

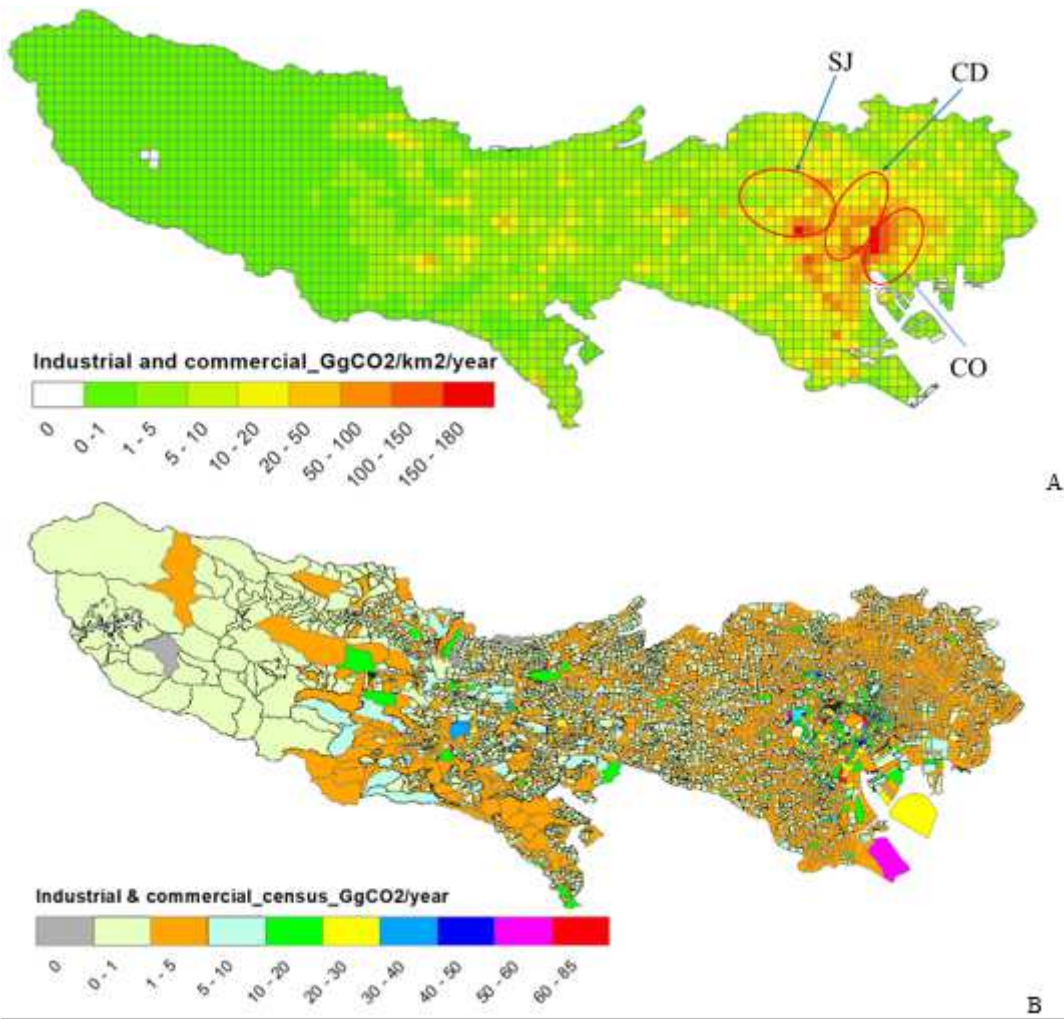


Figure 6

Map of emissions from the industrial and commercial sector with (A) 1 × 1 km mesh, unit: Gg CO₂ km⁻² yr⁻¹; (B) 5,318 economic census areas, unit: Gg CO₂ yr⁻¹. The municipality boundary for the area with the highest annual emissions (up to 82.2 Gg CO₂) is marked in cyan.

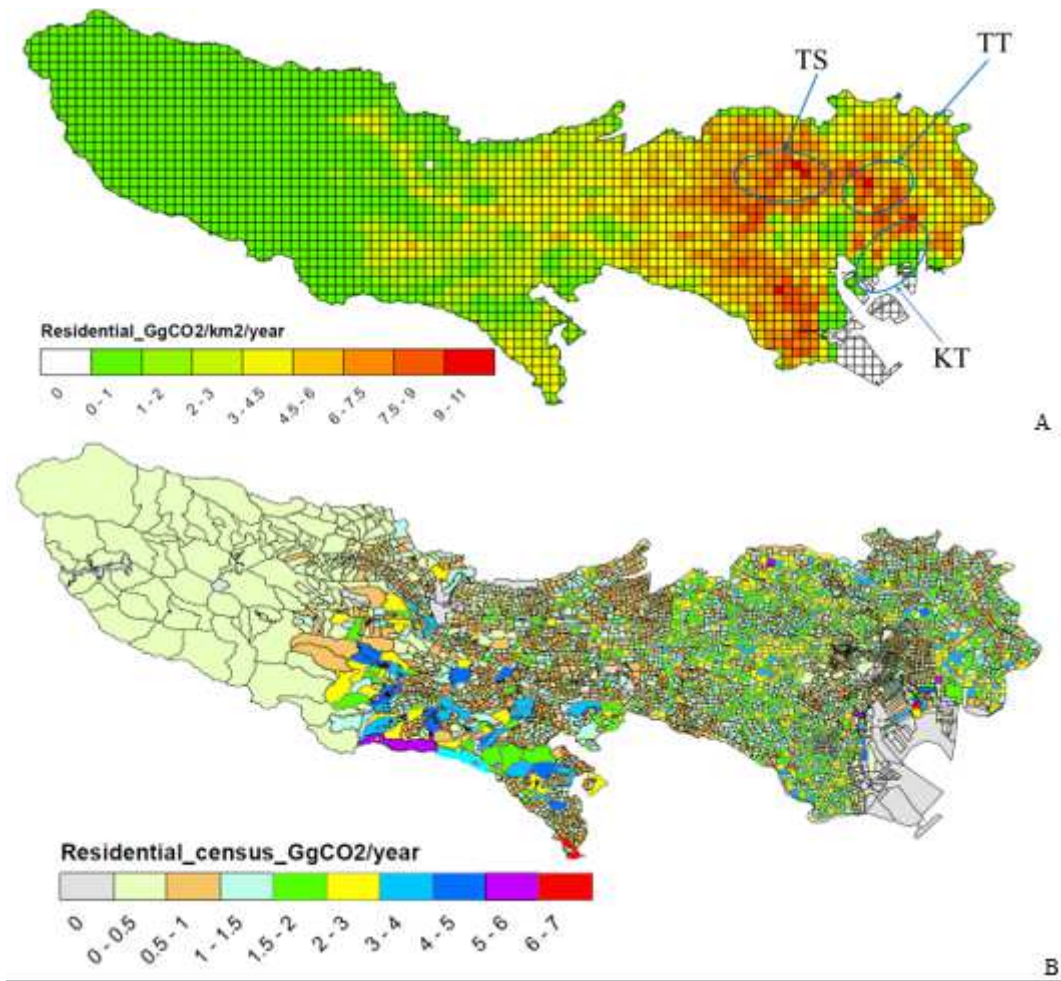


Figure 7

Map of emissions from the residential sector with (A) 1×1 km mesh, unit: $\text{Gg CO}_2 \text{ km}^{-2} \text{ yr}^{-1}$; (B) 5,578 population census areas, unit: $\text{Gg CO}_2 \text{ yr}^{-1}$. The municipality boundary for the area with the highest annual emissions (up to 6.6 Gg CO_2) is marked in cyan.

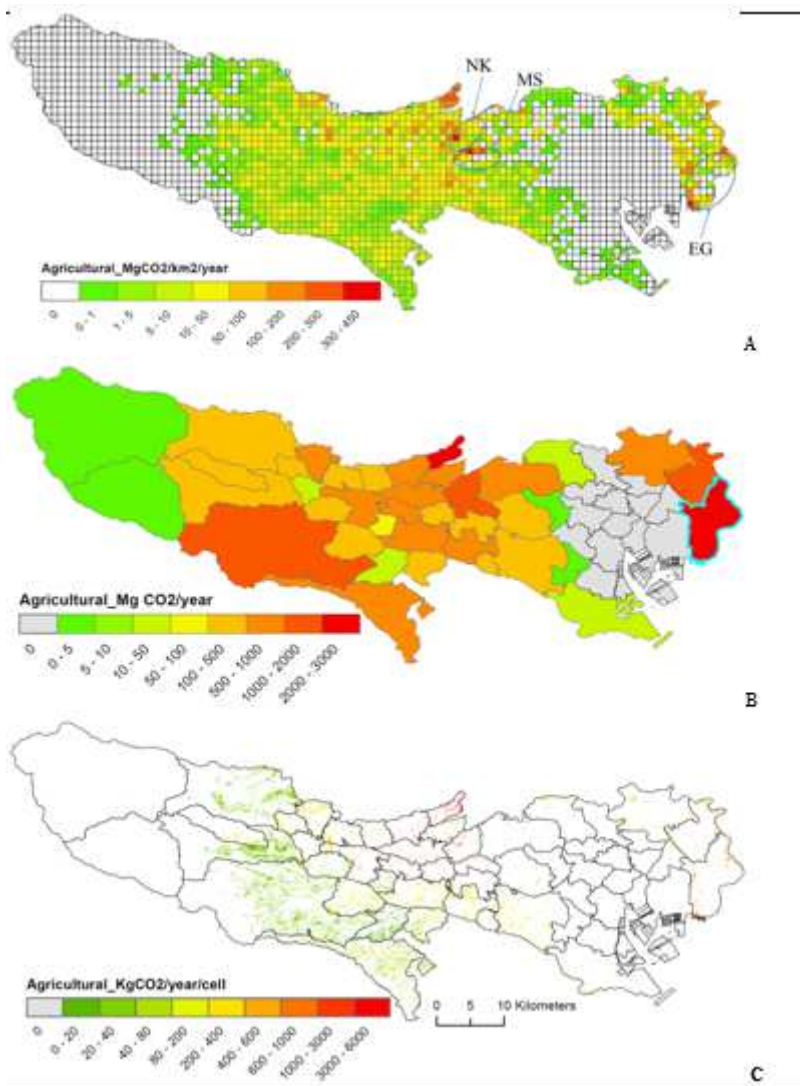


Figure 8

Maps of emissions from the agricultural machine use sector with (A) 1 × 1 km mesh, unit: Mg CO₂ km⁻² yr⁻¹. (B) 62 municipalities, unit: Mg CO₂ yr⁻¹. The area with the highest annual emissions (2,765 Mg CO₂ yr⁻¹) is marked in cyan. (C) high-spatial-resolution map on a grid with cell size of 10 × 10 m, unit: Kg CO₂ yr⁻¹ per cell.

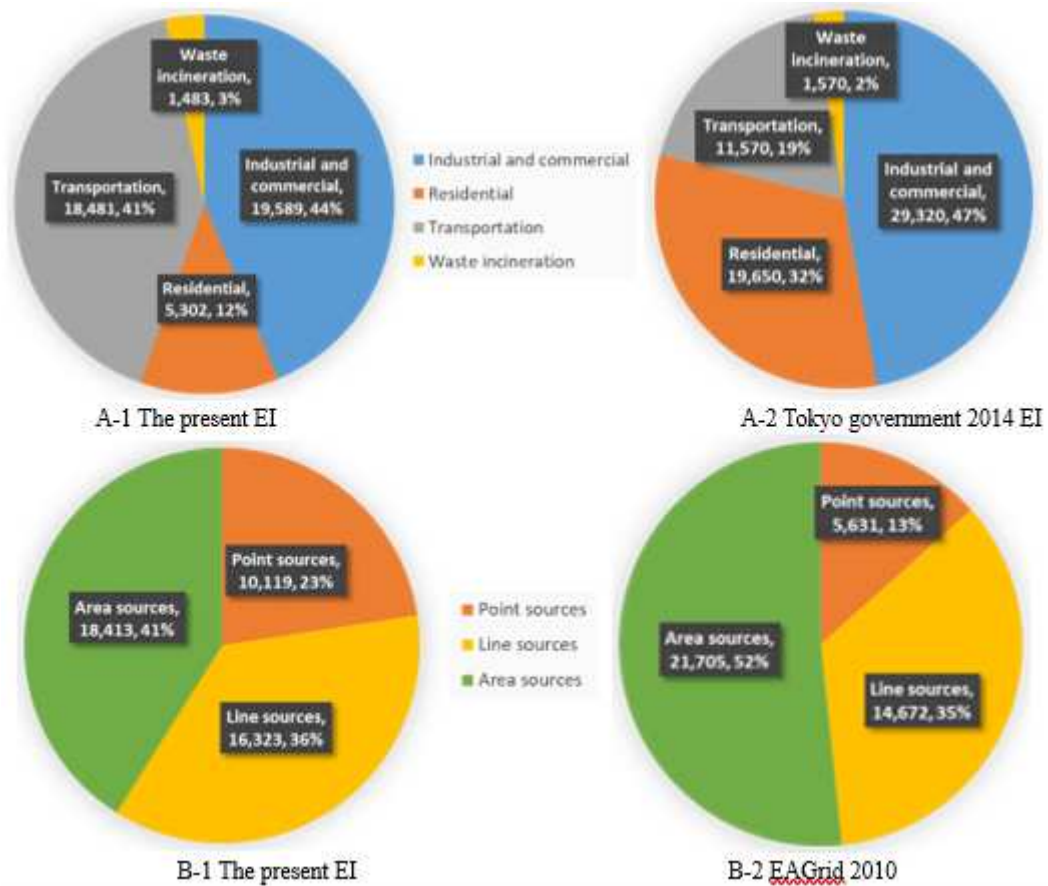


Figure 9

Comparisons on annual CO₂ emissions in Tokyo between the present EI (A-1) and Tokyo government 2014 EI (A-2), and between the present EI (B-1) and EAGrid-Japan 2010 (B-2). Unit: Gg CO₂. Note: In A-1, the industrial and commercial category includes emissions from the industrial and commercial sector and the electricity generation sector. The transportation category includes emissions from the road transportation, civil aviation, and waterborne navigation sectors. In A-2, the transportation category includes emissions from the railway, road transportation, civil aviation, and waterborne navigation sectors. In B-2, point sources include power plants, waste incineration plants, vessels, and aircrafts. Line sources refer to road transportation. Area sources include residential and commercial combustion equipment, factory and building boilers, off-road transportation, open burning, and facilities without identified locations.

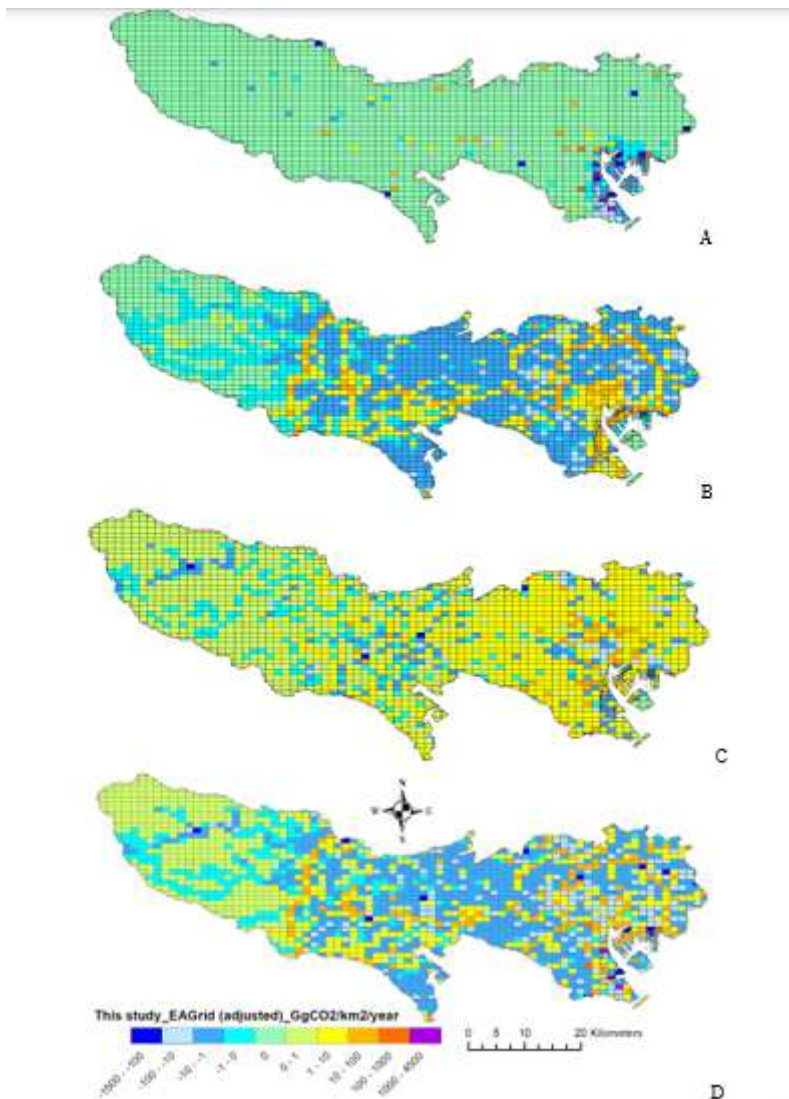


Figure 10

Differences in emissions between the present EI and 2010 EAGrid-Japan EI at a resolution of 1 × 1 km for: (A) point sources, (B) line sources, (C) area sources, and (D) all sources. Unit: Gg CO₂ km⁻² yr⁻¹. (Difference = emissions from the present EI – 2010 EAGrid-Japan EI, after adjustment of EAGrid emissions, as described in the text.).

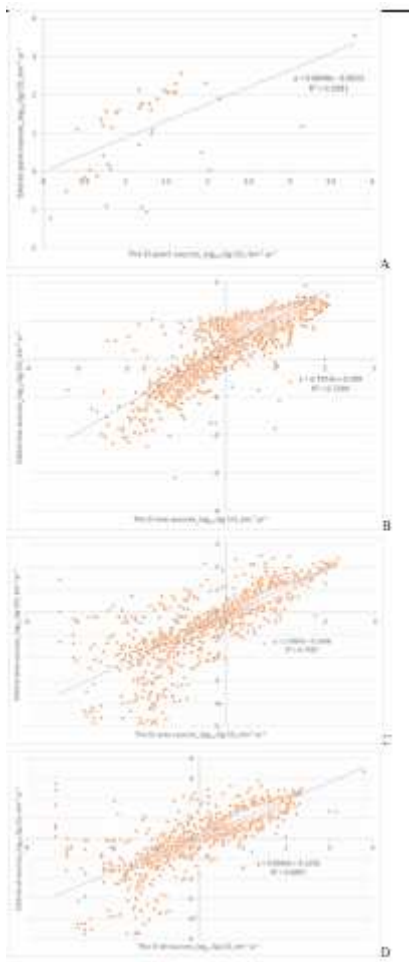


Figure 11

Scatter plots of gridded emissions by source types between the present EI and EAGrid for: (A) point sources, (B) line sources, (C) area sources, and (D) all sources. Unit: \log_{10} Gg CO₂ km⁻² yr⁻¹.

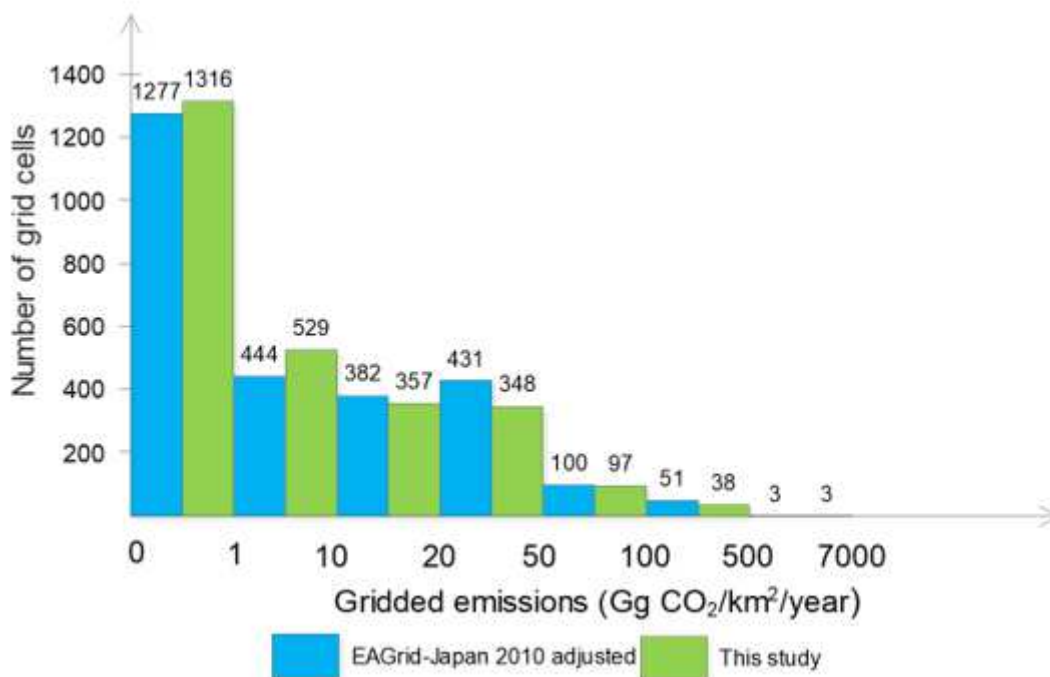


Figure 12

Frequency distribution of gridded emissions (Gg CO₂ km⁻² yr⁻¹) for this study (green) and EAGrid-Japan 2010 adjusted (blue). n = 2,688.

Supplementary Files

This is a list of supplementary files associated with this preprint. Click to download.

- [Supplement.docx](#)